Design of a self-aligning 3-DOF actuated exoskeleton for diagnosis and training of wrist and forearm after stroke

J. Houdijn Beekhuis*, Ard J. Westerveld*, Herman van der Kooij*†, and Arno H.A. Stienen*‡
*Laboratory of Biomechanical Engineering, University of Twente, Enschede, NL
†Biomechanical Engineering, TU Delft, NL
‡Physical Therapy and Human Movement Sciences, Northwestern University, Chicago (IL), USA
Corresponding author: arnostienen@gmail.com

Abstract—**Rehabilitation robotics provides a means of objectively quantifying patient condition before, during and after treatment. This paper describes the design and preliminary validation results of a novel rehabilitation device for the human wrist and forearm.**

The design features two key aspects: 1) it performs dynamical self-alignment to compensate for misalignment of the human limb and 2) it assists movements within almost the full natural range of motion. Self-alignment is performed by a linkage of parallelograms that allows torque-driven actuation. Advantages are decreased user-device interaction forces and lower don/doff- and setup-times. The full natural range of motion in Flexion/Extension, Radial/Ulnar-deviation and Pronation/Supination allows patients to perform ADL-like exercises during training. Furthermore, in the current design the hand and fingers remain free to perform grabbing activities and the open structure provides simple connection to the patients limb.

Keywords–Rehabilitation robotics; self-alignment; self-aligning exoskeleton; wrist and forearm; diagnosis; training; stroke

I. INTRODUCTION

Stroke is currently regarded as the second cause of death in the Western world, and causes 10 percent of deaths worldwide. In up to 75 percent of stroke survivors physical or mental disabilities occur at onset of stroke [1]. Due to plasticity of the human brain it is possible to restore some motor functions of the upper extremities during rehabilitation [2], which allows patients to operate in Activities of Daily Living (ADL) with a higher degree of autonomy.

Current research at the University of Twente involves development of several solutions regarding robotic rehabilitation for the upper extremities after stroke. Projects Dampace [3] and Limpact [4] focus on exoskeletal, joint-level rehabilitation that supports and (actively) controls limb movements of the upper arm and shoulder. The MIAS-ATD [5] project focuses on end-point manipulation combined with electrical stimulation to support arm rehabilitation. The common objective is the generation of neurological and technical knowledge necessary for developing smart active therapeutic devices that are able provide patient specific therapy. However, current exoskeletons in this research group are not yet equipped for actuation and measurement of the more distal parts of the human arm. This

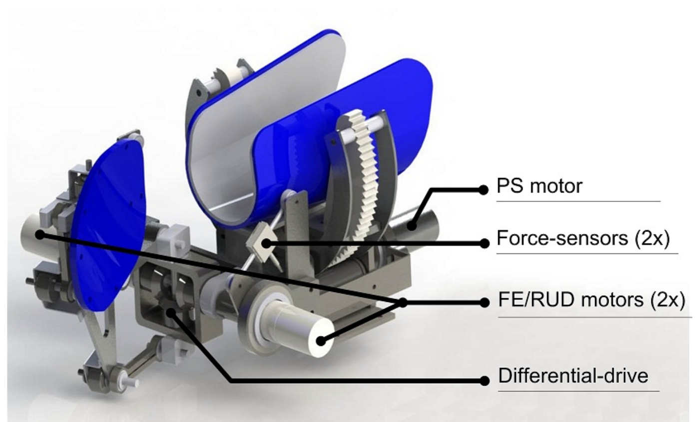

Fig. 1. The exoskeleton without a human limb attached. Flexion / Extension (FE) and Radial / Ulnar-deviation (RUD) both originate in the differential drive to which the parallelograms attach. The parallel system of FE and RUD is attached in serial to the rotational slider that performs Pronation and Supination (PS) of the hand, forearm and entire distal section of the device. Force sensors (of which only 1 shown here) measure provided motor-torques.

paper describes a design to extend the functionality of the current projects to the wrist and forearm.

Several designs for upper extremity rehabilitation have been presented by other research groups, including the RiceWrist [6][7], MAHI and MAHI II [8] and the Supinator Extender [9]. Whereas the Ricewrist and MAHI are based on a parallel system to drive wrist motions the Supinator Extender uses a serial approach. Despite large structural differences they have one thing in common: Once connected to a human limb careful alignment of mechanical and human joints is necessary to prevent residual forces causing false sensor readings and patient discomfort [10]. Most of the current designs of wrist robots do not acknowledge the difficulties that arise when a human limb and an exoskeleton are not properly aligned.

The Limpact [4], MIT-Manus wrist robot [11] and the ESA Human Arm Exoskeleton[12][13] incorporate passive DOF which have a fully defined kinematic chain only when the human limb is in place. This development could greatly aid ease of use (although it complicates mechanical design) and

978-1-4673-6024-1/13/$31.00 ©2013 IEEE

decrease interaction forces and don/doff-time.

This paper describes a novel self-aligning 3 degrees of freedom actuated exoskeleton for wrist and forearm. The design dynamically adapts for misalignment thereby decreasing user-device interaction forces and don/doff-time. In addition to this it can provide assistance during training within the full natural range of motion of the wrist and forearm while its sensors objectively diagnose joint-condition. The device connects to the back of the hand so hand and fingers remain free to allow ADL activities with the device in place, and features an open structure for simple don/doff.

II. Background

Thorough understanding of human anatomy helps to create a design that respects natural limitations and abilities of the human joints. The axis of Pronation/Supination passes through the proximal head of the radius and the distal styloid process of the ulna, a line that can be prolonged towards the ring finger [14]. The anatomy of the wrist consists of 8 carpal bones connected to each other, the hand and forearm by ligaments that constrain undesired motion between the bones [15]. The gliding planes within the wrist can be approximated by eccentric motion over an ellipsoid, as dictated by the radio-carpal joint [13]. During wrist movements, this complex anatomy reflects in its centers of rotation: the rotational axes of Flexion/Extension and Radial/Ulnar deviation are distally apart by 5 mm [15][14] to 20 mm [13]. Due to complex joint behavior axes of rotation are not fixed [16].

Because of these anatomical characteristics manual alignment of the wrist requires thorough, time-consuming observation or even the help of imaging devices. Also, constant adjustment during therapy makes for low repeatability over multiple therapeutic sessions [4][17], hence the need for dynamical self-alignment.

III. Requirements

Any mechanical addition to the body might feel unnatural to a certain extent, therefore the design follows several guidelines concerning the range of motion, the degrees of freedom and attachment to the body. This will allow the device to cope with the naturally present anatomical differences between individuals and ensure smooth user-device interaction and high ease of use. This should make interaction with the device feel as natural as possible.

A. Self-alignment and Degrees of Freedom

To allow smooth interaction with the motion of the wrist a carefully placed series of 6-DOF is needed [13]. When the device is attached to the wrist (and only then) it forms a closed kinematic loop allowing unambiguous actuation without restricting motion, within mechanical boundaries. In this design, three passive degrees of freedom allow the links of the parallelogram to translate into a new zero-force position whenever misalignment occurs [4], while three active degrees of freedom control joint-orientation.

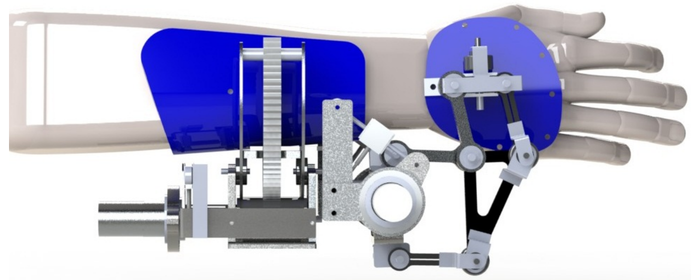

Fig. 2. Side view render of the Wrist and forearm Exoskeleton with a human arm in place. A linkage of parallelograms that enables 2-DOF self-alignment is attached to the back of the hand. The base of the Pronation/Supination slider can either be mounted to the fixed world or to an existing upper extremity exoskeleton.

B. Range of motion and motor torques

The device should allow for the natural range of motion of a healthy person without restrictions, so required ROM of the device is specified at 130 degrees in Flexion/Extension (wrist), 50 degrees in Radial/Ulnar-deviation (wrist) and 170 degrees in Pronation/Supination (forearm) [13][14][18][19].

Specified motor-torques are given in table I, requirements are based on findings about torques in ADL as given in [8][20], current designs with wrist function [14][18][19][20], and device-specific calculations.

TABLE I
Natural ROM and required Torques

Joint motion	ROM (deg)	Total (deg)	Torque (Nm)
Flexion / Extension	70 / 60	130	2
Radial / Ulnar-deviation	20 / 30	50	2
Pronation / Supination	80 / 90	170	4

IV. Design

The wrist exoskeleton is designed using DS Solidworks and is built as a proof of principle prototype, Fig. 1 and Fig. 2 show a CAD-model of the device. The majority of parts has a 2D outline which allows low-cost production by means of laser-cutting. Its dimensions are (length·width·height) 320·260·160 mm, and the entire prototype including electrical parts, produced out of stainless steel and aluminum weighs around 1 kg. Although low mass of the device is important in later stages no specific weight optimization has taken place for this prototype, which functions mainly as a proof of principle for actuation and torque-transmission. The device will be placed stationary on a table or, if the weight is further optimized, could be attached to aforementioned Limpact Exoskeleton for further testing. Therefore the majority of the weight will be held by either the fixed world or an upper-arm exoskeleton. Although this is not currently incorporated, gravity compensation of the parallelogram-linkage could cancel further impedance making the device suitable for patients with low strength.

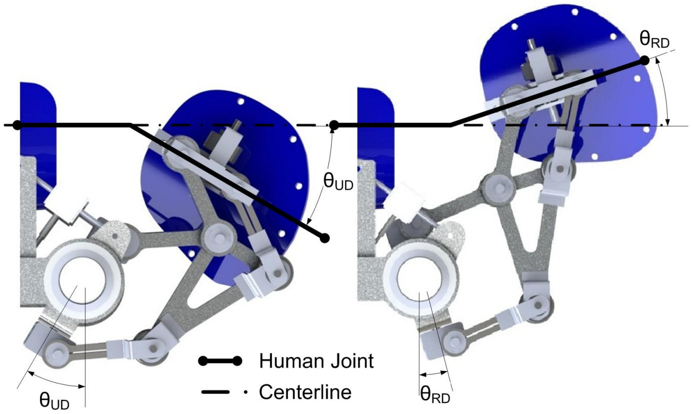

Fig. 3. Side view of the torque-driven motion in Radial/Ulnar-deviation actuated through motion of the parallelograms. Rotation of the motors is passed through the linkage to the wrist in a 1:1 ratio. In this visualization θ_{RUD} is split into θ_{RD} and θ_{UD}. Decoupling of translation and rotation allow the linkage to automatically align to the rotational center of the wrist, which in the illustrated motion is located proximal of the hand-cuff.

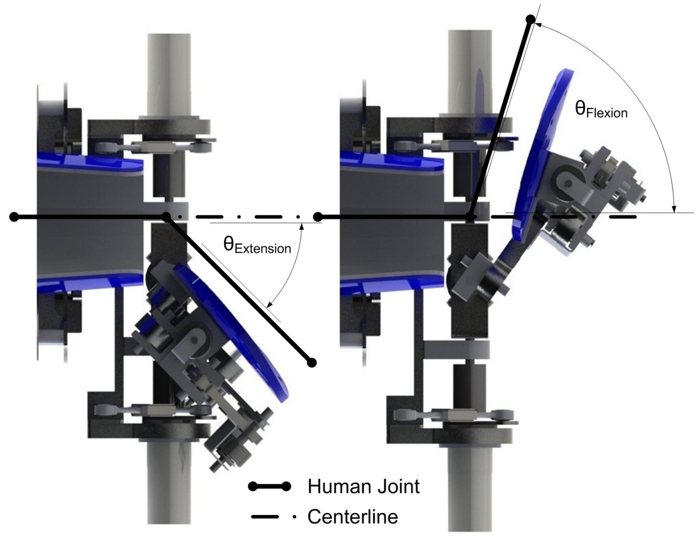

Fig. 4. Top view of the Wrist Exoskeleton performing Flexion/Extension (FE) along its full range of motion, positioned in 45 degrees of extension (left image) and 70 degrees of flexion (right image). Here θ_{FE} is split into $\theta_{Flexion}$ and $\theta_{Extension}$. Visible in grey on both sides the Pololu 25Dx56L motors.

A. *Differential transmission*

A differential-drive transmission (see Fig. 1) allows two motors to drive a 2-DOF rotation. Similar transmissions have been previously applied by the 'iCub' Humanoid Robot [21] and the InMotion Wrist Robot [19], among others. A differential drive has two advantages: Firstly the motors cooperate allowing motor torques to be added together, which allows for smaller motors. Secondly it features a parallel transmission rather than serial transmission where the one motor would support the weight of the next. In this proof of principle Pololu 172:1 Metal Gearmotors, type 25Dx56L will be used. These motors come with 48 CPR Encoder, that allows for a resolution of 0.04 degree per count at the output axle.

Kinematics are straight-forward as gears are implemented in a 1:1 ratio. Equations of motion at the output axle of the differential are:

$$\theta_{RUD} = \frac{(\theta_R + \theta_L)}{2} \quad (1)$$

$$\theta_{FE} = \frac{(\theta_R - \theta_L)}{2} \quad (2)$$

where θ_{RUD} and θ_{FE} respectively represent movements in Radial/Ulnar-deviation and Flexion/Extension, and θ_R and θ_L represent rotation of the left and right motor. In both directions the power of both actuators is the sum of the power of the individual motor, or:

$$T_{RUD} = (T_R + T_L) \quad (3)$$

$$T_{FE} = (T_R - T_L) \quad (4)$$

where T_{RUD} and T_{FE} respectively represent Radial/Ulnar-deviation torque and Flexion/Extension-torque.

B. *Torque and force-driven actuation*

The design uses two types of actuation. A system of parallelograms allows pairwise application of forces during Radial and Ulnar-deviation (Fig. 3), and decouples rotations from translations (Fig. 6). This torque-driven actuation has become independent of positional misalignment, body-supplied reaction forces or torques applied to other joints [4]. A pairwise application of forces requires two connections per limb segment.

Flexion/Extension (Fig. 4) is provided in the conventional method which most exoskeletons use to drive joint movements, where a single force is applied to the end of a limb segment, which rotates this segment around the human joint axis. The distance between the rotational center of the joint and the applied force determines the actual torque within the limb and needs to be known. A single connection to the limb suffices.

The direct application of torques has an advantage for the smaller range of motion required for Radial/Ulnar-deviation, but was found that in this design case the force-driven actuation is better suited to drive the large range of motion required for Flexion / Extension. Tests with the functional prototype will provide further insights into these aspects, and allow for thorough comparison.

C. *Radial and ulnar-deviation*

Radial and Ulnar-deviation (RUD) are performed in a torque-driven manner, when motors are driven in equal directions, see Fig. 3. This allows the motor-torque to be directly translated to applied joint-torque. The torque sensors are able to measure hand- and device-weight to compensate for gravitational forces of the hand and parallelogram. Joint-

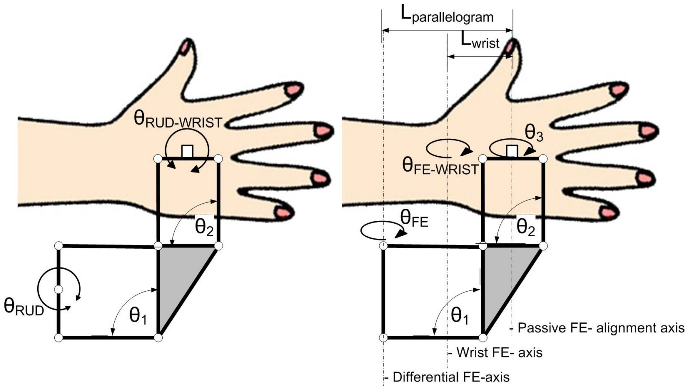

Fig. 5. Schematic views of the parallelograms attached to the back of the hand. Important characteristics during Radial/Ulnar deviation (left) and Flexion/Extension (right) are indicated. Because of the force-driven actuation during FE $l_{parallelogram}$ and l_{wrist} are determined to calculate exact torques on the wrist. Each of the corners in the parallelogram hinges freely, as illustrated by the white dots. The rotations are registered by sensors: θ_1 to θ_3 are monitored by potentiometers, θ_{FE} and θ_{RUD} are determined by the motor-encoders.

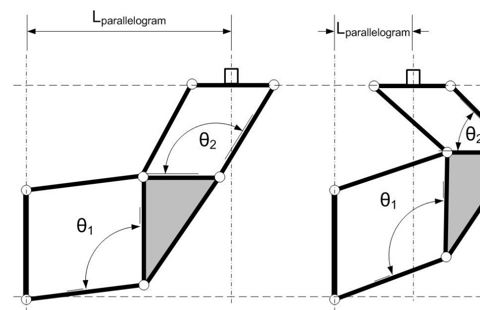

Fig. 6. Example of decoupled rotations and translations during horizontal alignment: the center of the cuff stays at the same level and no rotation of the wrist joint is induced. The linkage can be independently translated hence and forth, while θ_1 and θ_2 are monitored by potentiometers to determine $l_{parallelogram}$.

orientation is directly coupled to motor-rotation and monitored by the motor-encoders, while joint-position is released to self-alignment during motion. Fig. 5 schematically illustrates the rotations involved. In RUD this means that:

$$\theta_{RUD} = \theta_{RUD-WRIST} \tag{5}$$

D. Flexion and extension

Flexion and extension are performed by driving the motors in opposite directions, which results in a swiveling motion of the wrist structure, see Fig. 4. During rotation the parallelograms compensate for misalignment. Force-driven actuation lies at the basis of this motion, so the resulting torque-arm is measured by potentiometers. Combining these readings with motor-torque values leads to the applied joint torque:

$$T_{wrist-FE} = \frac{l_{wrist}}{l_{parallelogram}} * T_{FE} \tag{6}$$

where $T_{wrist-FE}$ is the torque applied to the wrist joint, l_{wrist} is the horizontal distance between the rotational center of the wrist joint and the vertical axis of connection to the hand, and $l_{parallelogram}$ represents the horizontal distance between the differential's vertical axis and the vertical axis of the hand connection, as schematically illustrated in Fig. 5.

$l_{parallelogram}$ depends on current configuration of the linkage and is obtained by measuring link-orientation within the parallelogram by means of two centrally placed potentiometers that measure θ_1 and θ_2. Because link-lengths are known, simple geometric relations suffice to determine end-point position.

When the wrist's FE-axis and devices differential-axis are aligned it can be assumed that l_{wrist} will be equal to $l_{parallelogram}$ and the torque-ratio will equal 1. This alignment is performed manually to determine torques in [16]. If the wrist's FE-axis does not match the FE-axis of the differential, the linkage allows passive translation to a position in which no residual forces on the hand or sensors remain [4], as seen in Fig.6. During movement a third potentiometer measures wrist rotation with respect to parallelogram rotation (θ_3 in Fig. 5). Along with current measurements for $l_{parallelogram}$ the actual position of the rotational center of the wrist and the resulting l_{wrist} is calculated.

During wrist rotations in FE the rotation of passive joint θ_3 is involved, and relations between motor- and wrist-rotations are given by:

$$\theta_{FE-WRIST} = \theta_{FE} + \theta_3 \tag{7}$$

Where $\theta_{FE-WRIST}$ is the rotation of the human wrist joint, θ_{FE} is the rotation of the differential and θ_3 is the rotation of the passive FE-joint.

E. Pronation and supination

Pronation and Supination are performed around the virtual pivot point of a 240 degree arc, see Fig. 7. The forearm rotates around a virtual axis through its center as is the case in [8][20][22][23], among others. Although this does not exactly correspond to the anatomical axis exact alignment is not critical [13] and the aforementioned designs report positive results. A horizontal laser-cut slot pushes the top-bearings onto the arc to provide pre-tension, which is adjustable by a set of screws (not illustrated here) to allow fine-tuning of the 'smoothness' of the movement. A single Pololu 75:1 Metal Gearmotor, type 25Dx54L that comes with 48 CPR Encoder will be used, this allows for 0.015 degrees per count resolution of the arc's rotation. A set of HPC synthetic gears (types HPC ZG-1.5-96-ZPG and ZG-1.5-14-ZG) will be modified to drive the motion.

F. Sensors

All three motors are equipped with a Futek LSB-200 force-sensor that is eccentrically mounted to the housing at a specified distance from the motor axle. The torques applied to the system can therefore be calculated by measuring reaction forces on the motor housing, resulting in a clean torque-determination at the output axle of the gearbox.

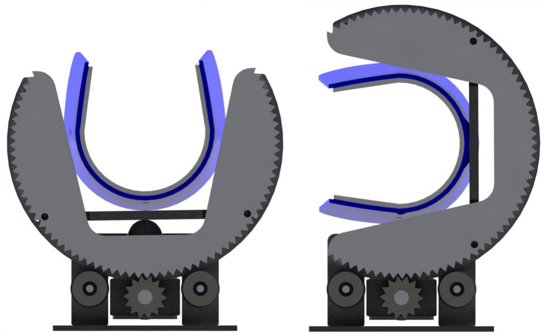

Fig. 7. Front view section cut of the device performing Pronation / Supination. Left: Neutral position, right: 90 degrees Supination. The virtual center of rotation is positioned slightly below the center of the human arm.

Three potentiometers monitor position of the parallelogram linkage, to determine the force-arm during FE. Motor-encoders provide positional information of the differential and wrist-joint orientation.

G. Connection to arm, hand and fixed world

The patients arm will be secured into the cuffs by means of Velcro straps. The open mechanical structures allow for simple placement of the human limb, without the need for guiding it through rings or other narrow structures that might complicate the procedure. The hand-piece connects to the back of the hand by means of two Velcro straps at both ends of the cuff, so the hand is left free and patients are able to perform ADL tasks during training. Depending on patient's condition it might still be required to secure the fingers either straight or flexed during parts of the therapy. This could be achieved by introducing a splint or cylindrical bar, respectively.

H. Control system

For testing purposes an Arduino Due (with 84Mhz ARM processor) based system with Pololu Motor Shields will function as processing unit of the sensor data. A single driver can drive two 3A DC motors, and will simplify control of the Pololu 25Dx56L motors of the differential. A second driver will drive Pronation / Supination. The drivers support Pulse Width Modulation (PWM) to control motor speeds, braking of the motors and measures motor-currents.

V. VALIDATION

A prototype has been built to allow mechanical and functional validation of the design, see Fig. 8 and Fig. 9. Preliminary mechanical validation has been performed, main points of interest are ROM, alignment and the influence of this alignment on ROM. Subjective qualities like comfort of the cuffs and comfort of performing motions with the device are also subject of interest.

The range of motion is tested in pure FE, RUD and PS by fitting a limb and measuring maximal angular deviation while changing limb position within a range of four centimeters. Results are given in table II. The vertical force exerted on the hand is measured with a spring balance, and amounts to

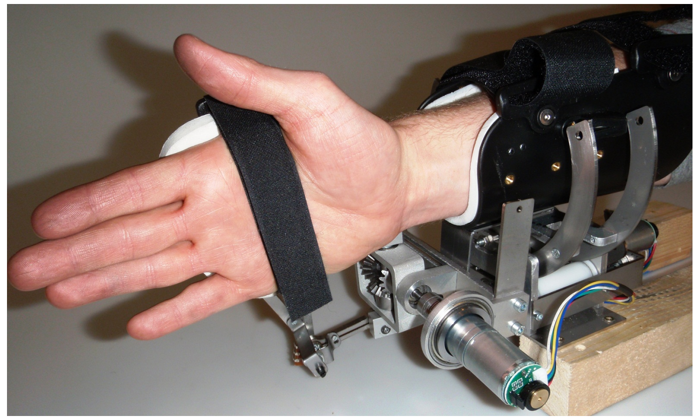

Fig. 8. Proof of principle prototype that is used for evaluation of the concept. Don/doff can be performed in under ten seconds with the Saebo cuffs and Velcro straps. One of the Pololu motors with encoder is visible in the front.

3.0 N, or a torque of 0.15 Nm around the wrist joint. Fitting the device to a healthy subject is performed in less than ten seconds.

TABLE II
ROM (DEGREES) FOR ALIGNMENT OFFSET (CM), FROM -2 CENTIMETERS PROXIMAL TO +2 CENTIMETERS DISTAL MISALIGNMENT

Motion	ROM -2	ROM -1	ROM +0	ROM +1	ROM +2
F/E	80 / 45	80 / 50	80 / 55	80 / 55	80 / 60
R/UD	20 / 15	20 / 20	20 / 25	15 / 35	15 / 35
P/S	80 / 80	80 / 80	80 / 80	80 / 80	80 / 80

The overall maximal ROM of the device is found when the parallelograms' position is neutral (90 degrees) during fixation. This can be easily established visually when the device is fitted to the patient. When compared to table I it can be seen that the device closely resembles the natural ROM, but does not always meet the requirements. No problems are expected because of this light deviation, but a closer look will be taken at further increasing the ROM by a simple redesign of the relevant parts. When the device is switched off the patient will only feel gravitational forces of the hand cuff and parallelograms. When motors are active the torque is cancelled out by the parallelograms, and the 3.0 N force translates to within the wrist joint. The currently used Saebo cuffs are comfortable during both don/doff and use, but may slightly slip during RUD, unless the Velcro straps are tensioned to uncomfortable levels during prolonged wear. Changing cuff-type will probably solve this. FE and PS are performed well. Overall the device allows for close to natural, smooth motion.

Further functional evaluation will comprise the measurement of passive wrist and forearm joint stiffness and the comparison of this data to values found in literature. For a final design a closer look could be taken at mass-reduction and cosmetic aspects.

VI. CONCLUSION

Details of the mechanical design of a novel self-aligning 3-DOF wrist and fore-arm exoskeleton have been presented.

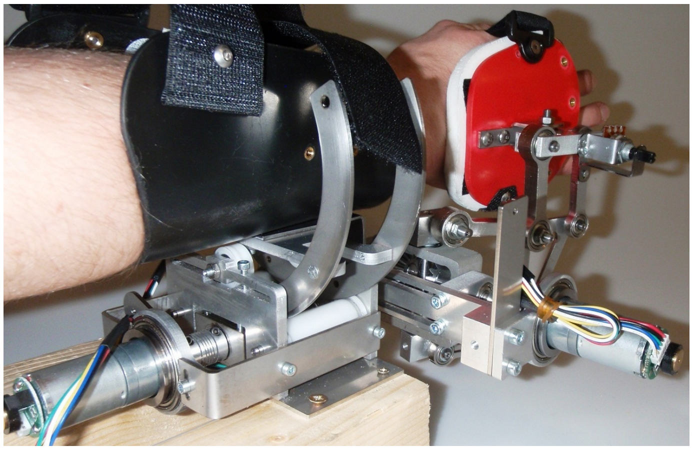

Fig. 9. Rear view of the prototype, showing the pre-tensioned flexible slot that allows adjustments for smooth slider motions. Visible on the right one of the potentiometers that will determine paralellogram positioning during motion.

This proof of principle focuses on actuation of the DOF and transmission of torques between actuators and the human limb. Current exoskeletons in this research group are not yet equipped for actuation and measurement of the more distal parts of the human arm and most of the current designs of wrist robots elsewhere do not acknowledge the difficulties that arise when a human limb and an exoskeleton are not properly aligned.

This exoskeleton adapts dynamically for misalignment whilst decreasing user-device interaction forces and has a don/doff-time of around 10 seconds. It can assist and objectively measure wrist and fore-arm movements. The hand and fingers of the patient remains available for grabbing motions when attached to the exoskeleton. The exoskeleton is able to assist in movements within almost the full natural range of motion, 130 degrees in Flexion/Extension (FE), 45 degrees in Radial/Ulnar-deviation (RUD) and 160 degrees in Pronation/Supination (PS). The exoskeleton comprises a parallel system to provide FE and RUD, driven by two motors that are coupled by a differential. A serially attached system drives PS. Additional sensors measure applied motor torques. The design is 'open' which allows the hand and arm of the patient to be placed with ease, without the need of guiding (potentially spastic) patients through narrow ducts.

We expect that the current device will further help extend the knowledge currently available in the field of upper extremity rehabilitation robotics for neurological disorders, by taking the effects of self-alignment and a natural ROM into account.

References

[1] P. Duncan, "Stroke disability," *Physical Therapy*, pp. 399–407, 1994.

[2] S. Charles, H. Krebs, B. Volpe, D. Lynch, and N. Hogan, "Wrist Rehabilitation Following Stroke: Initial Clinical Results," *9th International Conference on Rehabilitation Robotics, 2005. ICORR 2005.*, pp. 13–16, 2005.

[3] A. Stienen, "Dampace: dynamic force-coordination trainer for the upper extremities," in *2007 IEEE 10th International Conference on Rehabilitation Robotics*, vol. 00, no. c, 2007.

[4] ——, "Self-aligning exoskeleton axes through decoupling of joint rotations and translations," *Robotics, IEEE . . .* , vol. 25, no. 3, pp. 628–633, 2009.

[5] A. J. Westerveld, A. Kuck, A. C. Schouten, P. H. Veltink, and H. van der Kooij, "Grasp and release with surface functional electrical stimulation using a Model Predictive Control approach." *Conference proceedings : ... Annual International Conference of the IEEE Engineering in Medicine and Biology Society. IEEE Engineering in Medicine and Biology Society. Conference*, vol. 2012, pp. 333–6, Aug. 2012.

[6] M. O'Malley, A. Sledd, and A. Gupta, "The RiceWrist: A distal upper extremity rehabilitation robot for stroke therapy," *ASME International . . .* , 2006.

[7] Z. Kadivar, J. L. Sullivan, D. P. Eng, a. U. Pehlivan, M. K. O'Malley, N. Yozbatiran, and G. E. Francisco, "Robotic training and kinematic analysis of arm and hand after incomplete spinal cord injury: a case study." *IEEE ... International Conference on Rehabilitation Robotics : [proceedings]*, vol. 2011, p. 5975429, 2000.

[8] A. U. Pehlivan, O. Celik, and M. K. O'Malley, "Mechanical design of a distal arm exoskeleton for stroke and spinal cord injury rehabilitation." *IEEE ... International Conference on Rehabilitation Robotics : [proceedings]*, vol. 2011, p. 5975428, Jan. 2011.

[9] J. Allington, S. J. Spencer, J. Klein, M. Buell, D. J. Reinkensmeyer, and J. Bobrow, "Supinator Extender (SUE): a pneumatically actuated robot for forearm/wrist rehabilitation after stroke." *Conference proceedings : ... Annual International Conference of the IEEE Engineering in Medicine and Biology Society. IEEE Engineering in Medicine and Biology Society. Conference*, vol. 2011, pp. 1579–82, Jan. 2011.

[10] A. Schiele, "Ergonomics of exoskeletons: Objective performance metrics," *World Haptics 2009 - Third Joint EuroHaptics conference and Symposium on Haptic Interfaces for Virtual Environment and Teleoperator Systems*, pp. 103–108, 2009.

[11] L. Masia, H. Krebs, P. Cappa, and N. Hogan, "Whole-Arm Rehabilitation Following Stroke: Hand Module," *The First IEEE/RAS-EMBS International Conference on Biomedical Robotics and Biomechatronics, 2006. BioRob 2006.*, pp. 1085–1089.

[12] A. Schiele and G. Visentin, "The ESA human arm exoskeleton for space robotics telepresence," *. . . Intelligence, Robotics and Automation in Space*, 2003.

[13] A. Schiele and F. C. T. van der Helm, "Kinematic design to improve ergonomics in human machine interaction." *IEEE transactions on neural systems and rehabilitation engineering : a publication of the IEEE Engineering in Medicine and Biology Society*, vol. 14, no. 4, pp. 456–69, Dec. 2006.

[14] R. Gopura and K. Kiguchi, "Development of an exoskeleton robot for human wrist and forearm motion assist," *Industrial and Information Systems, 2007. . . .* , no. August, pp. 8–11, 2007.

[15] Y. Youm and a. E. Flatt, "Design of a total wrist prosthesis." *Annals of biomedical engineering*, vol. 12, no. 3, pp. 247–62, Jan. 1984.

[16] N. Rijnveld and H. Krebs, "Passive wrist joint impedance in flexion-extension and abduction-adduction," *. . . Robotics, 2007. ICORR 2007. IEEE 10th . . .* , vol. 00, no. c, pp. 43–47, 2007.

[17] M. Ergin and V. Patoglu, "ASSISTON-SE: A self-aligning shoulder-elbow exoskeleton," *Robotics and Automation (ICRA), 2012 . . .* , pp. 2479–2485, 2012.

[18] D. Williams, H. Krebs, and N. Hogan, "A robot for wrist rehabilitation," *Engineering in Medicine and . . .* , 2001.

[19] H. I. Krebs, B. T. Volpe, D. Williams, J. Celestino, S. K. Charles, D. Lynch, and N. Hogan, "Robot-aided neurorehabilitation: a robot for wrist rehabilitation." *IEEE transactions on neural systems and rehabilitation engineering : a publication of the IEEE Engineering in Medicine and Biology Society*, vol. 15, no. 3, pp. 327–35, Sep. 2007.

[20] J. C. Perry, J. Rosen, and S. Burns, "Upper-Limb Powered Exoskeleton Design," *IEEE/ASME Transactions on Mechatronics*, vol. 12, no. 4, pp. 408–417, Aug. 2007.

[21] W. M. Hinojosa, N. G. Tsagarakis, and D. G. Caldwell, "Performance Assessment of a 3 DOF Differential Based Waist joint for the iCub ? Baby Humanoid Robot," 2001.

[22] N. Hogan and J. Celestino, "Characterization and control of a robot for wrist rehabilitation," 2003.

[23] N. Yozbatiran, J. Berliner, C. Boake, M. K. O'Malley, Z. Kadivar, and G. E. Francisco, "Robotic training and clinical assessment of forearm and wrist movements after incomplete spinal cord injury: a case study." *IEEE ... International Conference on Rehabilitation Robotics : [proceedings]*, vol. 2011, p. 5975425, 2011.